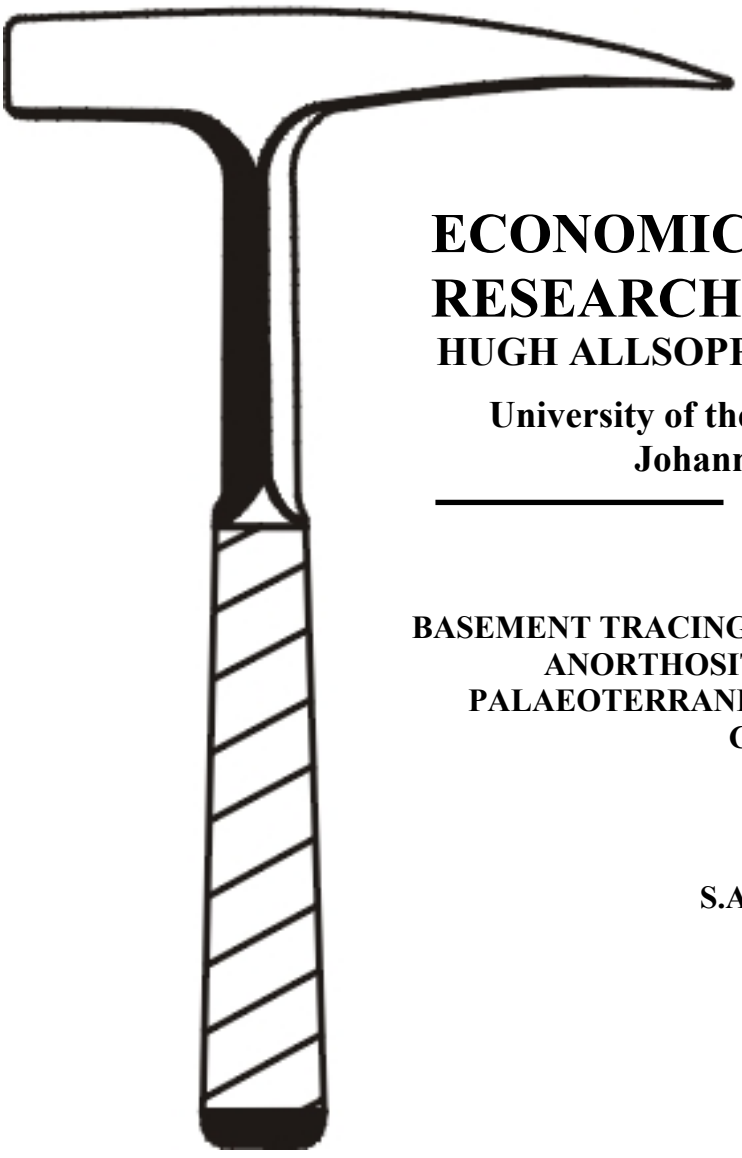

ECONOMIC GEOLOGY RESEARCH INSTITUTE

HUGH ALLSOPP LABORATORY

University of the Witwatersrand
Johannesburg

BASEMENT TRACING USING MID-PROTEROZOIC ANORTHOSITES STRADDLING A PALAEOTERRANE BOUNDARY, ONTARIO, CANADA

S.A. PREVEC

INFORMATION CIRCULAR No. 365

UNIVERSITY OF THE WITWATERSRAND
JOHANNESBURG

BASEMENT TRACING USING MID-PROTEROZOIC ANORTHOSITES STRADDLING A PALAEOTERRANE BOUNDARY, ONTARIO, CANADA

by

STEPHEN A. PREVEC

(Economic Geology Research Institute - Hugh Allsopp Laboratory, University of the Witwatersrand, Private Bag 3, P.O. WITS 2050, Johannesburg, South Africa)
e-mail: 006spa@cosmos.wits.ac.za

ECONOMIC GEOLOGY RESEARCH INSTITUTE
INFORMATION CIRCULAR No.365

December, 2002

BASEMENT TRACING USING MID-PROTEROZOIC ANORTHOSITES STRADDLING A PALAEOTERRANE BOUNDARY, ONTARIO, CANADA

ABSTRACT

Low-uranium, euhedral zircon grains were obtained from coarse-grained anorthositic rocks in two intrusions in Ontario, Canada. Assuming Grenvillian lower intercepts (at 1000 Ma), the St Charles and Mercer anorthosites give ages of 1245±120 Ma and 1244±5 Ma respectively. The former is from SHRIMP-generated data, the latter from "conventional" TIMS. The high errors for both methods are artifacts of the very shallow discordia line. These ages correlate with those of the Sudbury Dykes, 50 km to the north in the Superior Province, with granitoid emplacement further to the east in the Central Metasedimentary Belt, and with granulite facies metamorphism to the south. The dates and setting suggest that the two intrusions have experienced essentially identical geological histories. There are some differences in the extent of deformation (such that metamorphism varies from greenschist facies metamorphism to gneissose in both, but with more pervasive gneissosity in the Mercer Anorthosite). The mineralogical effects consist largely of hydration (saussuritisation and amphibolitisation), and should have had minimal effect on the incompatible trace element distributions and on Sm-Nd isotopic systematics.

The trace element geochemical signatures of the two intrusions are dominated by the effects of plagioclase accumulation, consistent with the petrographic evidence. Chondrite-normalised REE profiles display modest LREE-enrichment and pronounced positive Eu anomalies. The magnitude of the anomalies decreases with increasing REE abundance, consistent with variable contributions from trapped (intercumulus?) liquids. The samples are also characterised by high field strength element (HFSE)-depletion (Nb, Zr, Hf), consistent with this interpretation. There is, however, a consistent difference between the geochemistry of the two intrusions, whereby the Mercer Anorthosite displays higher trace element abundances, on average, and more LREE-enrichment, where $(La/Yb)_N$ ranges from 6 to 9 for the Mercer and around 2 to 4 for St Charles. This does not correlate with any systematic variation in REE- plot or spidergram anomalies. Likewise, the Sm-Nd isotopic system shows a similar distinction, whereby the Mercer samples give very consistent signatures with ε_{Nd}^{1240} values of -2.1 to -2.6, while those for St Charles are -3.9 to -6.5.

Assuming a similar upper-crustal evolution for the two intrusions, and given the suspected nature of the basement, the discrepancies between the two intrusions may be interpreted in terms of similar amounts of assimilation of two distinct lower crustal rock types during ascension through the crust. The St Charles Anorthosite would have ascended through relatively old radiogenic Archaean basement, which is relatively incompatible element poor, whereas the Mercer Anorthosite ascended through basement comprising a mixture of Archaean and Proterozoic material, with more incompatible-enriched and more isotopically juvenile signatures. This is consistent with the observations presented above and suggests that the apparent suture between Archaean foreland and an accreted Palaeoproterozoic arc represents a significant deep-crustal lineament, consistent with their interpretation.

This study supports the efficacy of the application of anorthositic rocks as sensitive samplers of the lower crust. This may be attributable to the fact that anorthosites represent mineralogically, and therefore geochemically, relatively simple systems (being largely monomineralic) and that the amount of crustal assimilation is small, and therefore does not "swamp" the host signature.

_____oOo_____

BASEMENT TRACING USING MID-PROTEROZOIC ANORTHOSITES STRADDLING A PALAEOTERRANE BOUNDARY, ONTARIO, CANADA

CONTENTS

_____oOo_____

Published by the Economic Geology Research Institute
(incorporating the Hugh Allsopp Laboratory)
School of Geosciences
University of the Witwatersrand
1 Jan Smuts Avenue
Johannesburg
South Africa
http://www.wits.ac.za/egru/research.htm

ISBN 1-86838-320-2

BASEMENT TRACING USING MID-PROTEROZOIC ANORTHOSITES STRADDLING A PALAEOTERRANE BOUNDARY, ONTARIO, CANADA

INTRODUCTION

The presence of an apparent basement suture in the Precambrian below the southern margin of the Superior Province in Canada has been identified, constrained, and refined over the last decade (e.g., Dickin et al., 1989, 1990; Holmden and Dickin, 1995; Guo and Dickin, 1996; Dickin, 1998a). This suture is defined at the surface by Late Archaean neodymium model-ages to the north and Early Proterozoic ages to the south of it. The boundary is also characterized by radiogenic Pb isotopic compositions (Dickin, 1998b). This isotopic break has been identified within the Grenville Province in Ontario and Quebec, occurring tens of kilometres to the south of and subparallel to the Grenville Front Tectonic Zone which defines the northern limit of that province. The Grenville Province, although defined by a characteristic 1000 Ma metamorphic overprinting age (Stockwell, 1969; Easton, 1986), has long been recognized as a collage of early- to middle-Proterozoic terranes along with reworked Archaean rocks (e.g., Rivers, 1997). The model-age boundary has been interpreted as a suture between Archaean foreland and an accreted Palaeoproterozoic arc (Dickin, 1998a).

The influence of adjacent and chronologically distinct basement terranes may be evaluated through the examination of mantle-derived intrusions or suites of intrusions which have passed through both. This has been demonstrated using anorthosites in the eastern Grenville where the geology is rife with both anorthositic and otherwise mafic intrusions, and major Precambrian terrane boundaries. Ashwal et al. (1986) examined suites of approximately contemporaneous (*c.*1400 to 1650 Ma) massif anorthosites and associated dykes emplaced into the Proterozoic Grenville Province and the Archaean Nain/Churchill Provinces to the north. Distinct differences in isotopic compositions of Nd (and Pb; Sr was relatively insensitive) were identified in the two suites. After a flirtation with interpreting this in terms of distinct mantle source characteristics (Ashwal and Wooden, 1983), ultimately this was attributed to less than 10% contamination of depleted mantle melts by crust of different ages appropriate to the respective basements, accompanied by fractional crystallization of the melts (Ashwal et al., 1986). Similarly, Emslie et al. (1994) examined a single anorthositic batholith (the Nain), beneath which passes the terrane boundary between the Nain (Archaean) and Churchill (reworked Archaean and Palaeoproterozoic) Provinces. They were able to distinguish between samples from either side of the boundary on the basis of their Nd isotopic signatures (but again, not with those of Sr). In this case, the fact that a single intrusion (even if polyphase) trangresses a terrane boundary allows subsequent isotopic distinctions to be most readily interpreted in terms of the basement (rather than in terms of source variations in space or in time).

In this study two anorthosites were identified to the west of Lake Nipissing, in the Grenville Province of Ontario. These intrusions share the same emplacement context, both intruding different parts of the (*c.* 1240 Ma) West Bay gneissic granitoid batholith. One anorthosite intrudes adjacent to the town of St Charles in the northwestern extremity of the batholith, and the other near Mercer Lake in the south central part of the batholith (Fig. 1). In this study the two anorthositic intrusions are examined using petrological data, zircon age dates, Sm-Nd isotopic data, and major and trace element geochemical data. The characteristics of the two bodies are then examined in the context of their setting on either side of the apparent underlying terrane suture.

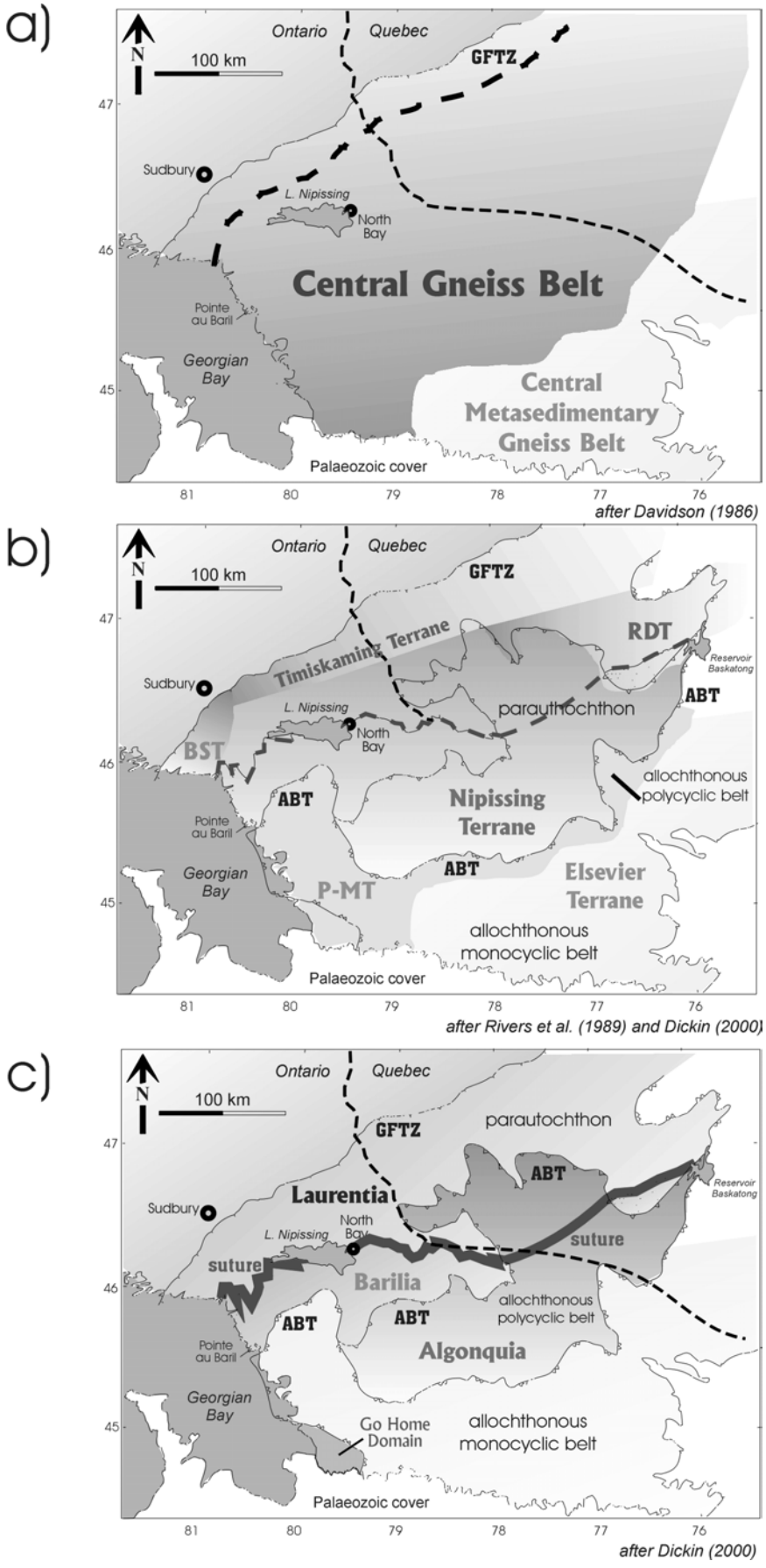

Figure 1: *Map of the western Grenville Province, Ontario, showing the evolution of terrane boundary interpretations (see text for discussion). Figure 1(a) is based on Wynne-Edwards (1972), 1(b) on Rivers et al. (1997), and 1(c) on Dickin (2000).*

GEOLOGICAL SETTING

The West Bay Batholith and the two anorthosites hosted within it lie within the Grenville tectonic province, approximately 50 km to the southeast of the city of Sudbury. This area lies within the structural subprovince of the Central Gneiss Belt or CGB (Wynne-Edwards, 1972), as depicted in Figure 1A. The CGB is overprinted along its northern margin by an approximately 20 km wide belt within which the effects of *c.* 1000 Ma north-to northwest-directed thrusting have been identified, known as the Grenville Front Tectonic Zone (GFTZ). This zone is constrained at its northern margin by the surface manifestation of the Grenville Front itself (Fig. 1).

Rivers et al. (1997) and Rivers and Corrigan (2000) have subdivided the Grenville Province into parautochthonous and allochthonous belts, with an intervening allochthon boundary thrust (ABT) belt. They identify three parautochthonous terranes in the northwestern CGB (Fig. 1B), consisting of the Beaverstone Terrane (characterised by Killarnean orogenic magmatism and distinctive aeromagnetic signatures) and the Timiskaming Terrane (consisting of reworked Archaean rocks) within the GFTZ, and the Nipissing Terrane to the south. The relatively poorly-defined Nipissing Terrane is characterised by 1500 to 1350 Ma granitoid gneiss sheets hosted by high-grade plutonic and supracrustal rocks, and is bounded to the south by the ABT, where the Parry Sound - Muskoka allochthon has been thrust northwards. These terranes are composed of a number of highly deformed, high grade (granulite to amphibolite facies) gneissic domains and subdomains bounded by high-strain, typically mylonitic zones (*e.g.*, Davidson, 1986 and references therein).

On the basis of Nd model age mapping, Dickin (2000) defined three new terranes within the parauthochthon (Fig. 1C). The northern terrane, Laurentia, is characterised by Neoarchaean model ages (*c*. 2700 Ma), and includes the GFTZ, along with the Beaverstone and Timiskaming Terranes of Rivers et al. (1997). Laurentia is defined along its southern margin by a distinct break in Nd model ages, to the south of which the Nd model ages are between 1900 and 1800 Ma. There is a transition zone to the north of the break, but the model ages there (around 2400 to 2500 Ma) are still distinctive from those to the south of it (e.g., Holmden and Dickin, 1994). The rocks with the Palaeoproterozoic ages (*c.* 1900 Ma) define a terrane identified as Barilia (Dickin, 2000). South and east of Barilia, but north of the ABT, is the remainder of the Nipissing Terrane, characterised by less uniform Palaeo- to Mesoproterozoic Nd model ages (1800 down to 1400 Ma), and has been termed Algonquia by Dickin (2000).

Dickin (1998) summarised three possible tectonic interpretations, which may relate to the model age break defining the northern margin of Barilia (and other terranes further east, defined by the same criteria, but beyond the scope of this study). Davidson et al. (1992) favoured prominent Killarnean (*c.* 1850 to 1750 Ma) orogenic activity (re. Beaverbrook Terrane) with minor Penokean (*c*. 1700 Ma deformation) overprinting. Feuton and Redmond (1997) advocated anorogenic Killarnean magmatism with minimal associated deformation. Dickin and McNutt (1990) proposed both Killarnean and Penokean orogenic activity. The former two models, as well as Rivers et al. (1997), do not recognise a major crustal suture within the Nipissing Terrane, while for Dickin and McNutt (1990), the northern boundary of Barilia represents a major crustal suture. Assembly of these terranes is interpreted to have occurred in the Palaeoproterozoic. As a result, the identification of the character (if not the existence) of the Barilia northern boundary has become an important issue in the understanding of the assembly of the thrust sheets which comprise the polycyclic allochthon of the Grenville Province.

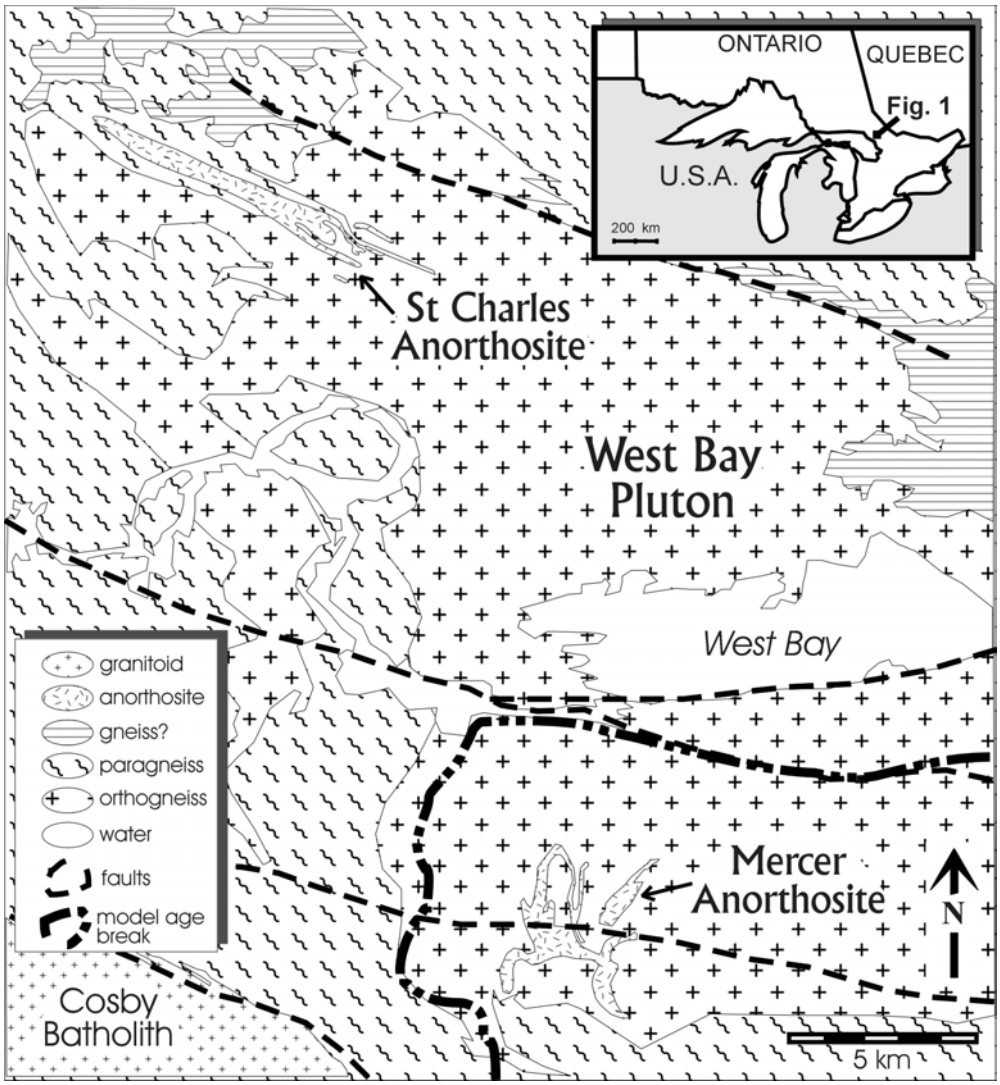

Figure 2: *Map of the Burwash area, showing the West Bay Batholith, the Mercer and St Charles anorthosites, and the location of the Barilia Nd model age boundary (Dickin, 2000).*

The northern terrane boundary of Barilia weaves in a generally east-west direction across high grade gneisses (Fig. 2), described by Lumbers (1975) as migmatitic hornblende- and/or biotite-bearing ortho- and paragneisses. The West Bay Batholith itself is migmatitic-to-gneissic quartz monzonite, with lesser hornblende-quartz monzonite and granodiorite. Lumbers (1975) also observed both xenoliths and concordant layers of metasediments within the granitoid, as well as evidence of apparent contamination of the granite by mafic rocks within it. He concluded that the batholith underwent a polydeformational history prior to the emplacement of the anorthosite suite, on the basis of two or more structurally defined events along with intense mineralogical recrystallisation.

METHODOLOGY

Samples 1-3 kg in weight were collected from surface outcrops and representative whole-rock extracts crushed to around 300 mesh. Major elements were determined by XRF at the Geological Survey of Canada (Ottawa, Canada), and trace elements by ICP-MS at the Geology Department, University of Cape Town, South Africa (Table 1). Sm-Nd isotopic analyses were carried out by the author at the Ministry of Northern Development and Mines (MNDM)

Geoservices Centre, Sudbury, Canada. Isotopic ratios were determined on a VG Sector 54 multi-collector thermal
ionization mass spectrometer (TIMS - see Table 2). Zircons were extracted from coarser-crushed material using a Wilfley Table and heavy liquids. The concentrate was sieved (the least magnetic fraction being obtained from Frantz isodynamic mineral separation at 1º tilt and 5º slope at maximum current of about 1.8 amps), and subsequently hand-picked for analysis. Zircons were analysed by a combination of conventional TIMS and ion microprobe (SHRIMP) methods. The analytical details are provided in Table 3.

PETROLOGY

St Charles Anorthosite

The St Charles samples are dominantly coarse-grained and anorthositic, consisting of 70 to 90 modal per cent andesine to labradorite plagioclase, the remainder consisting of altered femic minerals (mostly amphibole). Plagioclase is recrystallised, but relatively unaltered, displaying good albite and pericline twinning, although it may be as much as 25% sericitised in altered samples. Laths are preserved occasionally (e.g., SPA-89-12A) and very coarse-grained plagioclase may also be preserved. The plagioclase is altered in places to medium-grained epidote, usually in association with amphibole. In sample SPA-89-15, plagioclases show symplectic intergrowths along grain boundaries, and include coarser inclusions (exsolution?) which locally obscure the twinning.

Although intercumulus clinopyroxene may be preserved (e.g., SPA-89-18, 19 and Fig. 3A), it is usually entirely replaced by pale-green to olive-green to pale-brown pleochroic amphibole, which constitutes the dominant femic phase in these rocks. The amphibole does not typically preserve relic intercumulus textures, and is itself commonly altered along rims to chlorite, blue-green hornblende, epidote and calcite. Late biotite, associated with opaques (hematite and titanite), may pseudomorph amphibole (e.g., SPA-89-12B). These femic assemblages may be surrounded by "necklaces" of finer-grained, equigranular, pink almandine garnet (e.g., SPA-89-18; Fig. 3B). Titanite may also occur as rims around opaques (e.g., SPA-89-19), although both garnet and titanite may also occur as isolated grains within the feldspathic groundmass. Trace anhedral quartz may also occur (e.g., SPA-89-12A).

Table 1: Geochemical data for the St Charles and Mercer anorthosites

A. St Charles Anorthosite

Major Elements												
Sample	89-22	89-25	89-26	89-27	89-12B	89-13	89-15	89-16	89-18	89-19	89-20A	89-21
SiO2	50.10	51.40	51.70	53.00	51.30	51.20	51.70	52.10	51.90	52.30	52.40	51.70
TiO2	0.93	0.43	0.76	0.45	0.71	0.70	0.48	0.47	0.61	0.58	0.68	0.72
Al2O3	22.60	23.80	23.90	24.50	24.30	23.80	26.10	26.40	25.50	25.60	25.80	24.70
Fe2O3	2.43	1.93	2.26	1.95	2.21	2.20	1.98	1.97	2.11	2.08	2.18	2.22
FeO	4.11	2.67	3.10	1.49	3.05	3.15	1.37	1.29	1.70	1.64	1.10	2.32
MnO	0.08	0.05	0.08	0.06	0.07	0.06	0.04	0.04	0.05	0.05	0.04	0.06
MgO	3.82	3.00	2.93	1.07	2.49	2.74	1.79	1.54	2.06	1.72	1.21	2.39
CaO	9.63	9.27	9.85	8.86	10.21	10.06	10.58	10.91	10.42	10.52	10.51	10.42
Na2O	4.30	4.30	4.20	4.80	3.90	4.00	4.40	4.50	4.30	4.40	4.60	4.20
K2O	0.90	1.64	0.86	1.71	0.75	0.71	0.44	0.52	0.53	0.63	0.86	0.61
P2O5	0.22	0.10	0.16	0.13	0.12	0.08	0.09	0.12	0.15	0.15	0.13	0.14
H2O	1.00	1.30	0.80	0.80	0.70	1.00	0.60	0.60	0.60	0.50	0.80	0.50
CO2	0.00	0.00	0.00	0.00	0.00	0.10	0.10	0.00	0.00	0.00	0.00	0.10
Mg #	51.94	54.80	50.45	37.05	46.83	48.77	50.32	47.28	50.49	46.62	41.34	49.65

(all samples have SPA- prefix omitted; * are replicate analyses)

(Table 1 contd.)

B. Mercer Anorthosite

Trace Elements

Sample	89-22	89-25	89-26	89-27	89-12B	89-13	89-15A*	89-15B*	89-16	89-18	89-19	89-20A	89-21
Sc	9.11	4.67	9.10	6.59	9.19	12.1	4.02	5.46	3.56	5.42	5.86	6.47	8.75
V	88.2	43.0	70.0	11.1	79.7	90.6	38.8	63.4	35.3	48.7	58.6	64.0	69.7
Cr	81.4	21.3	20.7	37.8	51.7	54.0	14.1	27.4	15.8	13.7	16.6	11.2	20.3
Co	30.9	24.3	22.5	7.56	21.4	23.0	15.6	16.6	13.4	17.3	15.2	11.3	19.1
Ni	76.0	58.4	47.8	17.9	29.5	30.5	29.2	33.0	23.2	37.0	25.3	14.4	39.8
Cu	25.0	8.41	20.4	4.57	12.4	10.5	15.2	18.2	15.3	14.4	14.1	17.9	16.2
Rb	9.14	30.0	8.62	38.1	5.61	5.16	3.39	2.25	2.58	4.55	5.12	14.2	5.08
Sr	667	708	701	725	804	752	879	859	841	885	892	872	868
Y	10.8	4.23	10.9	14.7	7.40	7.03	4.21	3.95	4.02	6.69	6.94	6.72	7.59
Zr	11.9	8.04	10.8	22.4	4.59	11.6	6.82	3.73	3.34	5.62	6.18	6.52	7.45
Nb	4.73	1.04	4.56	8.77	3.06	2.48	1.95	1.74	2.32	2.91	5.26	3.05	2.61
Cs	0.13	0.38	0.18	0.62	0.15	0.14	0.076	0.052	0.077	0.10	0.10	0.26	0.10
Ba	356	541	259	518	365	253	316	307	304	362	362	347	354
La	8.94	4.91	9.19	14.8	5.92	5.97	5.03	3.77	4.22	6.48	6.58	6.42	6.59
Ce	19.9	10.2	20.4	32.7	15.1	13.0	10.6	8.83	10.1	14.4	15.1	14.3	14.9
Pr	2.59	1.28	2.63	4.02	2.00	1.70	1.34	1.09	1.24	1.85	1.94	1.83	1.93
Nd	11.1	5.32	11.2	16.4	8.60	7.30	5.58	4.83	5.44	8.06	8.53	7.96	8.52
Sm	2.30	1.00	2.31	3.39	1.79	1.55	1.05	0.97	1.06	1.63	1.72	1.62	1.76
Eu	1.06	0.68	1.06	1.32	1.10	1.07	0.84	0.75	0.76	0.99	0.96	1.01	1.01
Gd	2.23	0.92	2.12	3.04	1.65	1.50	0.97	0.91	0.95	1.50	1.54	1.49	1.65
Tb	0.32	0.13	0.32	0.45	0.23	0.22	0.13	0.13	0.14	0.21	0.22	0.21	0.24
Dy	1.97	0.77	1.93	2.65	1.38	1.32	0.79	0.79	0.82	1.24	1.31	1.25	1.40
Ho	0.39	0.15	0.39	0.52	0.27	0.26	0.15	0.15	0.16	0.24	0.25	0.24	0.28
Er	1.08	0.42	1.11	1.47	0.75	0.73	0.42	0.44	0.46	0.68	0.72	0.67	0.77
Tm	0.15	0.058	0.16	0.21	0.10	0.10	0.059	0.06	0.063	0.093	0.10	0.091	0.10
Yb	0.97	0.38	1.03	1.41	0.65	0.64	0.37	0.38	0.41	0.59	0.63	0.58	0.67
Lu	0.14	0.057	0.15	0.21	0.10	0.093	0.054	0.056	0.059	0.088	0.093	0.085	0.10
Hf	0.40	0.24	0.35	0.58	0.18	0.35	0.16	0.13	0.13	0.17	0.21	0.25	0.24
Ta	0.51	0.22	0.40	0.58	0.21	0.16	0.13	0.14	0.16	0.24	0.54	0.25	0.22
Pb	3.86	4.05	3.53	8.86	2.06	2.19	1.48	1.60	1.49	1.85	1.67	5.31	1.71
Th	0.84	0.39	0.95	2.85	0.29	0.32	0.27	0.18	0.23	0.35	0.37	0.37	0.37
U	0.23	0.069	0.33	1.34	0.075	0.093	0.075	0.052	0.067	0.092	0.10	0.10	0.10
La/Sm	2.402	3.020	2.454	2.688	2.039	2.385	2.956	2.390	2.449	2.456	2.357	2.442	2.309
Sm/Yb	2.560	2.874	2.442	2.607	2.968	2.636	3.043	2.743	2.832	2.975	2.949	3.042	2.846
La/Yb	6.149	8.681	5.993	7.009	6.052	6.288	8.994	6.556	6.933	7.306	6.953	7.428	6.571

TABLE 2: Sm-Nd isotopic data for the St Charles and Mercer anorthosites

Unit	Sample #	Sm *(ppm)*	Nd *(ppm)*	Sm/Nd	$^{147}Sm/^{144}Nd$	$^{143}Nd/^{144}Nd$	ε_{Nd}^{0}	ε_{Nd}^{1240}	$f_{Sm/Nd}$	T_{CHUR} *(Ma)*	T_{DM} *(Ma)*
Mercer	SPA-89-22	2.248	10.682	0.094	0.1272	0.511966	-13.11	-2.08	-0.3534	1471	1896
Mercer	SPA-89-25	1.099	5.707	0.175	0.1164	0.511863	-15.12	-2.37	-0.4082	1469	1848
Mercer	SPA-89-26	2.294	11.263	0.089	0.1231	0.511905	-14.30	-2.62	-0.3741	1515	1914
Mercer	SPA-89-27	3.062	15.299	0.065	0.1210	0.511906	-14.28	-2.26	-0.3851	1470	1868
St. Charles	SPA-89-12B	1.821	8.752	0.114	0.1257	0.511727	-17.78	-6.53	-0.3608	1950	2288
St. Charles	SPA-89-13	1.564	7.130	0.140	0.1326	0.511883	-14.73	-4.68	-0.3221	1811	2205
St. Charles	SPA-89-15	1.101	5.258	0.190	0.1266	0.511871	-14.97	-3.85	-0.3564	1664	2053
St. Charles	SPA-89-16	1.272	6.345	0.158	0.1211	0.511831	-15.75	-3.85	-0.3842	1624	1997

TABLE 3: U-Pb zircon isotopic data for the St Charles and Mercer anorthosites

ID	$^{207}Pb/^{235}Pb$	1 sig	1 sig %	$^{206}Pb/^{238}Pb$	1 sig	1 sig %
St. Charles						
1	2.207	0.080	3.62	0.1992	0.0040	2.01
2	2.312	0.110	4.76	0.2065	0.0042	2.03
3	2.330	0.077	3.30	0.2051	0.0041	2.00
4	2.267	0.078	3.44	0.2059	0.0041	1.99
6	2.262	0.065	2.87	0.2038	0.0040	1.96
7	2.356	0.073	3.10	0.2099	0.0040	1.91
8	2.207	0.087	3.94	0.2046	0.0040	1.96
Mercer						
AA	2.051	0.1477	7.20	0.1932	0.0033	1.70
AB	1.903	0.2036	10.70	0.1894	0.0045	2.40
BA	2.323	0.0023	0.10	0.2078	0.0002	0.08
BB	2.315	0.0023	0.10	0.2073	0.0002	0.09
AC	1.801	0.0036	0.20	0.1736	0.0002	0.11
C	2.298	0.0025	0.11	0.2060	0.0002	0.09
DA	2.339	0.0024	0.10	0.2089	0.0002	0.09
DB	2.321	0.0026	0.11	0.2078	0.0002	0.10

Mercer Anorthosite

The Mercer samples consist largely of well-preserved, recrystallised, coarse-grained plagioclase, and are similar in texture and mineralogy to the St Charles intrusion. The plagioclase may be moderately sericitised and/or epidotised, and albite and pericline twinning is well-preserved, indicating sodic andesine compositions. Pale-green to dark-green amphibole comprises most of the remainder of the rock, variably altered to red-brown biotite, which is invariably displays a strong foliation. Assemblages of opaques plus serpentine and hydrous iron oxides appear to represent orthopyroxene breakdown. Accessory minerals include scattered medium-grained euhedral-to-subhedral garnet, apatite, epidote and opaques.

In summary, both anorthosites exhibit largely recrystallised textures, with peak metamorphic mineralogy consistent with amphibolite facies metamorphism of what were likely orthopyroxene- and ilmenite-bearing anorthosites. The garnet and titanite alteration around amphibolitised pyroxenes and iron oxides, respectively, are suggestive of a prograde event, rather than simple post-emplacement cooling. Post-peak metamorphism (whether prograde or retrograde) accounts for the late saussuritisation and sericitisation. The Mercer Anorthosite samples reflect more extensive deformation in the form of pervasive foliation of secondary biotite.

GEOCHEMISTRY

The major element compositional range of the two anorthosites is essentially identical, although some degree of compositional variation is evident, consistent with minor modal variations. All samples contain between 50 and 53 wt.% SiO_2, and Al_2O_3 around 25 wt.% (Table 1), consistent with massif-type anorthosites elsewhere (e.g., Ashwal, 1993). These are distinct from the more noritic or gabbroic rocks associated with anorthosites elsewhere, which are characterised by lower silica, alumina and calcium, and higher magnesium abundances, reflecting the increase in pyroxene content relative to plagioclase.

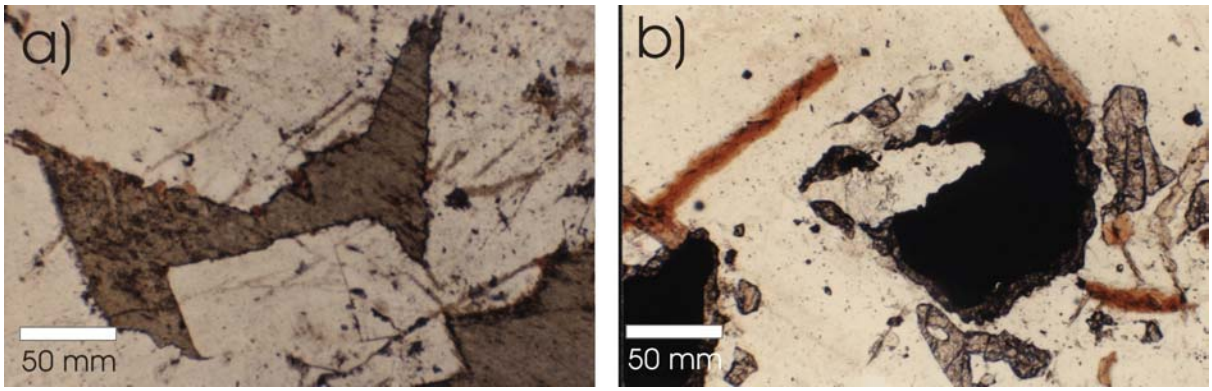

Figure 3: *Petrologic evidence for (a) relic igneous textures, showing intercumulus clinopyroxene with primocrystic plagioclase, and (b) prograde metamorphism, showing garnet necklaces around oxide (see text for discussion).*

Similarly, anorthositic rocks from layered mafic intrusions, such as the Stillwater or Bushveld complexes, typically contain lower silica contents (around 48-50 wt.%) and higher alumina (28-32 wt.%) and calcium (12 to 15 wt.%), as summarised by Ashwal (1993). On an AFM ternary plot, massif-type anorthositic rocks typically define trends lying within the calc-alkaline field (Fig. 4A). The trends also typically reflect variation in alkali content along lines of approximately constant iron/magnesium ratio. This is distinct from either the tholeiitic-type trends, where the variation reflects mainly changes in alkali-iron ratio, with relatively little variation in magnesium or calc-alkaline trends, which are dominated by alkali-magnesium variation (Irvine and Baragar, 1971). Of the small number of samples collected, most of the Mercer Anorthosite samples contain slightly less calcium and more magnesium than do the St Charles samples (Fig. 4B). Normative feldspar (plagioclase plus orthoclase, which is not present as a modal mineral) comprises between about 85 to 92% of the rock, with a calculated plagioclase anorthite content corresponding to An_{51-59} (sodic labradorite).

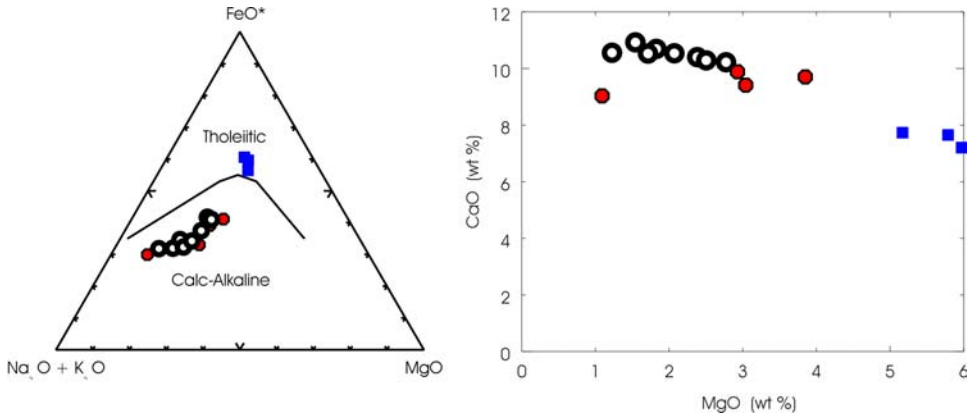

Figure 4**:** *AFM and Ca-Mg plots; open circles are St Charles, closed are Mercer, and the squares are Sudbury Dykes (for reference see text).*

The trace element composition of these samples is also characteristic of plagioclase cumulates. Chondrite-normalised REE profiles (Fig. 5A) show LREE abundances between 5 and 50x chondrite and HREE abundances of 2 to 6x chondrite, with prominent positive europium

anomalies. No samples show negative Eu anomalies. Primitive mantle-normalised spidergrams (Fig. 5B) show enrichments in Sr and Eu and depletions in the high field strength elements (HFSE), U, Nb, Ta and Zr, consistent with plagioclase accumulation. The Mercer Anorthosite samples are, on average, slightly enriched in the incompatible (and compatible) trace elements relative to the St Charles suite, as illustrated in both the REE profiles and spidergrams.

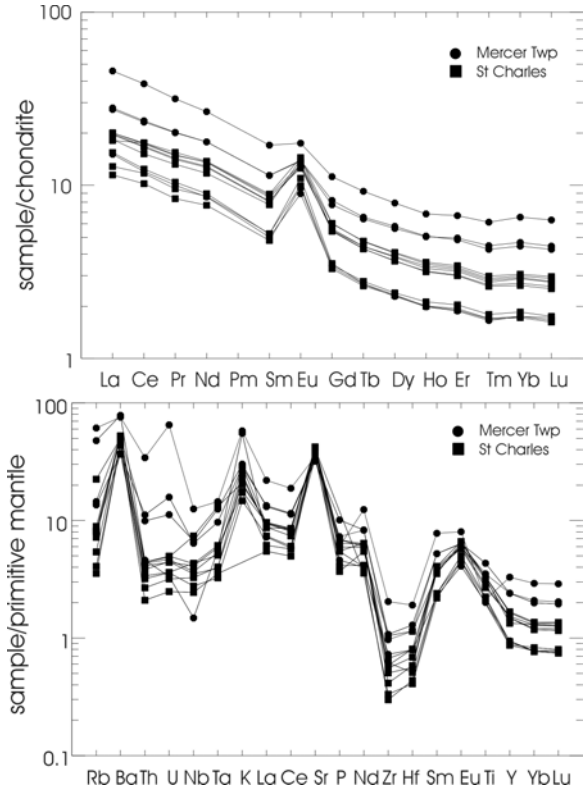

Figure 5: *REE and trace element spidergram profiles*

GEOCHRONOLOGY

St Charles Anorthosite

Sample SPA-89-14 is a plagioclase-amphibole-bearing, weakly epidotised gabbro-anorthosite, sampled from the northwestern end of the intrusion, near the town of St Charles (UTM zone 17, 544175E, 5134250N). The zircon yield was very poor, such that a 15 to 20 kg sample yielded less than 0.1 mg of zircon. The zircons were anhedral, equant to stubby prismatic, clear, colourless grains (Fig. 6A). Zoning was observed in some grains, but internal structure and fracturing was generally absent. The zircons therefore show no obvious physical signs of inheritance and are morphologically typical of anorthositic zircon (*cf.*, van Breemen et al., 1986). SHRIMP U-Pb isotopic analysis on eight spots (no more than one spot per any individual zircon grain) produced a cluster of points around concordia with an average $^{207}Pb/^{206}Pb$ age of 1206± 36 Ma (2σ).

Mercer Anorthosite

Sample SPA-89-22 was obtained from one of the northern extensions of the intrusion (UTM zone 1, 556850E, 5113100N), and is a relatively unaltered, albeit recrystallised rock. It is not quite anorthositic, *sensu strictu*, consisting of about 80 modal per cent andesine with lesser

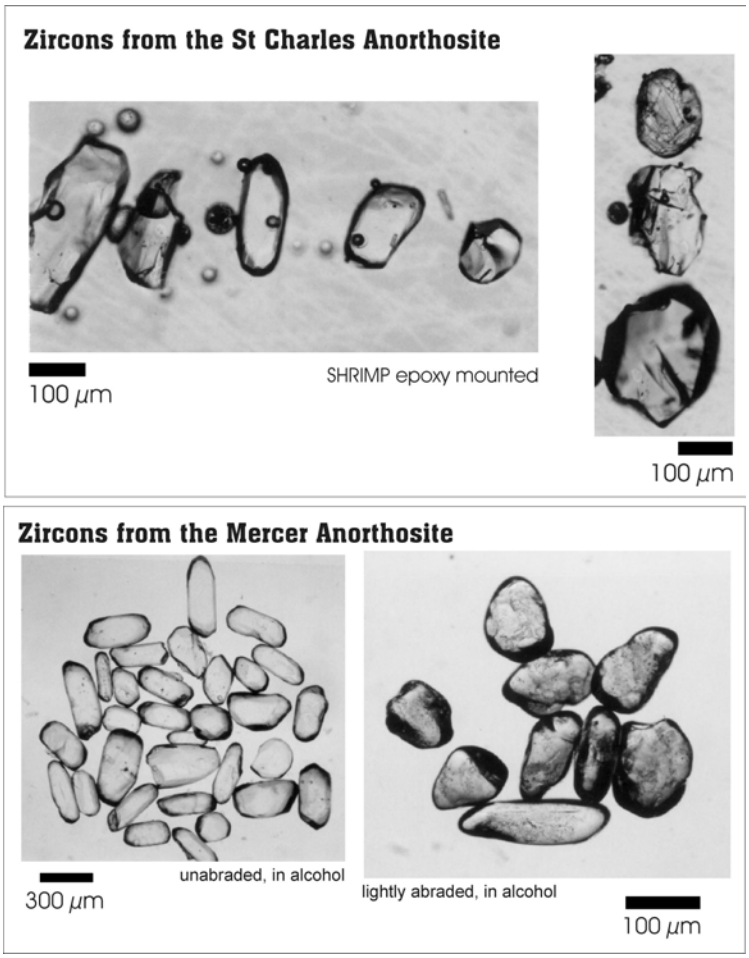

Figure 6: *Zircon photomicrographs for St Charles and Mercer anorthosites.*

amphibole, biotite, garnet and apatite. Four zircon populations were identified, consisting of extremely clear, subhedral grains with rounded tips (population A), coarser, often fragmented, anhedral, darker and more fractured grains (population B), a coarser-grained, slightly cloudy equivalent of population A (C), and inclusion- and fracture-rich, anhedral grains (D), shown in Figure 6B. Eight fractions of one to three grains each were analysed after moderate abrasion. Population A were characterised by very low uranium contents (less than 7 ppm U), and produced relatively low-precision "Grenvillian" ages around 1100 Ma (Table 3). Inclusion of all eight
fractions resulted in a lower intercept of 863 ± 26 Ma and an upper intercept of 1233.5 ± 4.4 Ma (2σ).

Sm-Nd ISOTOPE GEOCHEMISTRY

Four samples from each intrusion were analysed for Nd isotopic composition and Sm and Nd abundance. The results are presented in Table 2 and displayed in Figure 7. The data are shown on an isochron diagram, and while the data are loosely constrained between reference isochrons of about 1400 and 950 Ma, neither data set demonstrates closed system behaviour. It is apparent

that the two intrusions are showing evidence of distinct initial isotopic compositions. One St Charles sample, SPA-89-12B, falls well below the other seven samples. As its Sm/Nd ratio is consistent with the others, the most likely interpretation is that the Nd isotopic composition has been modified (rather than for example, remobilisation of the REE resulting in significant secondary HREE enrichment).

Initial ε_{Nd} values (Table 2) for the St Charles Anorthosite, calculated for *c.* 1240 Ma, range between -3.9 and -6.5. The Mercer Anorthosite samples show a consistent signature of ε_{Nd}^{1240} between -2.1 and -2.6, all within analytical imprecision of one another.

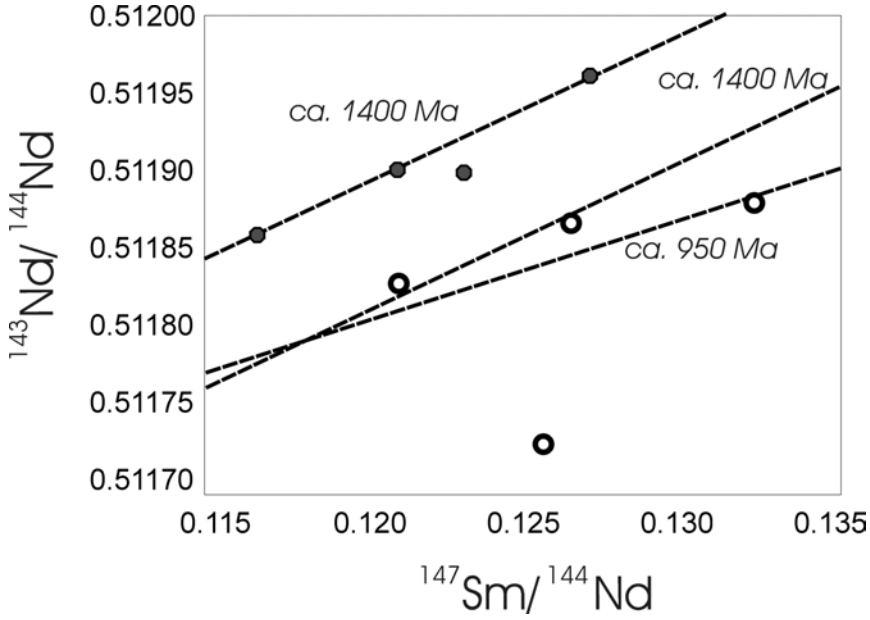

Figure 7: *Sm-Nd isochron diagram for the anorthosites.*

DISCUSSION

Age dates and tectonic context

The U-Pb age dates, as presented above, are of reasonable precision, but must be considered as relatively poorly constrained. The age for the St Charles intrusion must be modified by application of a meaningful lower intercept. The intrusion has been affected by a high-grade metamorphic event which can only be associated with Grenville-aged, northwest-directed thrusting. "Grenville" ages from pegmatites and high-grade metamorphism range around 1000 ± 20 Ma in the immediate area (North Bay to French River), as summarized by Easton (1986). The 863 Ma lower intercept age for the Mercer Anorthosite correlates with no reported geological event in the area, and is most likely an artifact of a shallow discordia and subsequent lead loss, and is probably geologically meaningless. While application of any *c*. Grenvillian lower intercept age produces contemporaneous upper intercept ages for the two intrusions (producing an upper intercept of 1231 ± 71 Ma if the lower intercept from the Mercer is used to anchor the St Charles data), a 1000 Ma lower intercept age has been assigned on the basis of the existing data. This results in ages of 1245 ± 48 Ma for the Mercer Anorthosite and 1244 ± 120 Ma for the St Charles Anorthosite (Model 1 solutions from Ludwig, shown in Fig. 8 A, B). The precisions are poor as a result of slight discordance in all grains, combined with a shallow

discordia line in the former case, and large error ellipses (from SHRIMP data) and shallow discordia, in the latter case. The ages now have very poor precision, but better constraints on their accuracy.

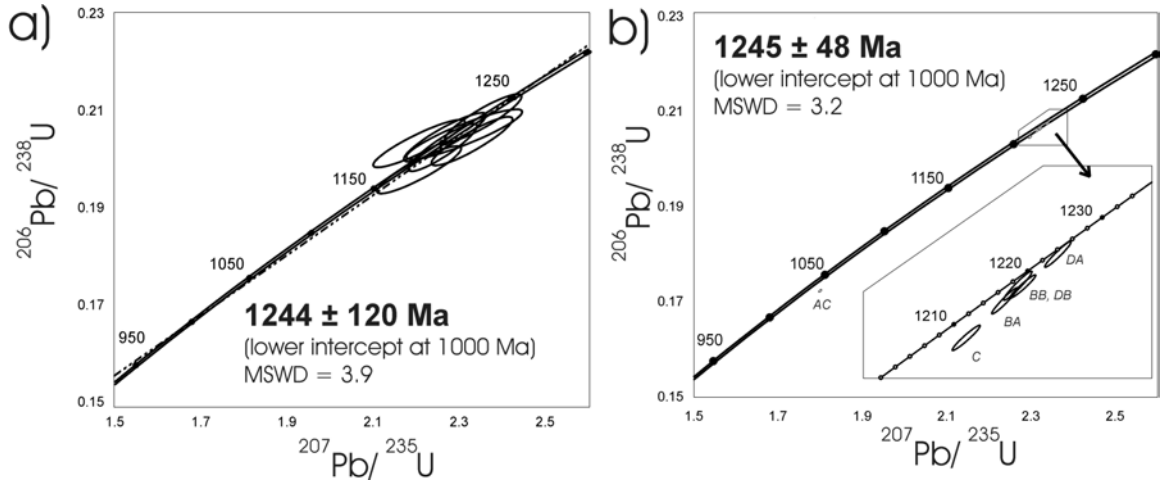

Figure 8: *U-Pb concordia diagrams for Burwash anorthosites, constrained to 1000 Ma lower intercepts (see text for discussion).*

Despite the very poor precision, the observation that the centroids of the two ages agree very well (regardless of the choice of lower intercept, as long as they are the same for each intrusion) suggests that the two intrusions can be reasonably assumed to have essentially identical emplacement ages. In the vicinity, *c.* 1240 Ma ages correlate with a 1244 +4/-3 Ma age for the Mulock granite batholith, 60 km to the northeast at the other end of Lake Nipissing. An unpublished age of *c.* 1240 Ma for the West Bay Batholith (from the Royal Ontario Museum) remains unconfirmed. These ages also correspond to granulite facies metamorphism near McKellar, in the Central Gneiss Belt about 100 km to the south, and to the Sudbury Dyke Swarm, about 50 km to the north, one member of which has been dated at 1238.5 ± 4 Ma (Krogh et al., 1987). The Sudbury swarm has been identified with either an aulacogen relating to a northeast-southwest-trending rift zone further south, along the current trend of the St Lawrence River, as a "Sudbury Ocean" (Fahrig, 1987), or alternatively somehow related to Grenvillian collision (as summarised by Osmani, 1991).

On the basis that these two anorthosites have intruded the same granitoid at the same time, it seems not unreasonable to expect similar geochemical and isotopic characteristics from the two intrusions. Instead, although all samples are geochemically dominated by the effects of plagioclase accumulation, there are clear differences between the trace element and isotopic compositions of the two intrusions. Geochemically, the Mercer intrusion shows incompatible trace element enrichment, with smaller negative Eu anomalies relative to the St Charles intrusion. The Mercer samples are also slightly more magnesian, suggesting a slightly larger component of trapped evolved liquid (as opposed to calcic plagioclase cumulate). On the basis of an even smaller database than this study, Simmons and Hansen (1978) suggested a plagioclase-rich, mantle-derived REE-rich parent magma, from which plagioclase accumulation and various amounts of trapped liquid (5 -10% for the St Charles; 30-50% for the Mercer) have produced the observed geochemistry. This is consistent with the inverse correlation between Eu anomaly and total REE content, and inferred relatively high REE abundances in the associated liquid and therefore in the parent magma. The petrographic evidence also indicates plagioclase primocrysts with later intercumulus clinopyroxene, consistent with a high - alumina (basaltic) parent (e.g., Prevec, 2000). A comparison of the REE patterns in the anorthosites with patterns modelled for plagioclase-only fractionation from a Huronian-type parent suggested

a more basaltic parent liquid (Prevec, 1993) rather than an anorthositic one, consistent with suggestions of a high-alumina basaltic parent for massif anorthosites (e.g., Ashwal, 1993).

Constraining cumulate-liquid mixtures on the basis of mass balance calculations of this nature are heavily dependent on the choice of partition coefficients (and the choice of parent magma). Phinney and Morrison (1990) provided partition coefficients for calcic plagioclase which are lower than previously derived values by factors ranging from two (for Eu), three to four for the LREE, and up to ten times lower for the HREE. Clearly, the choice of partitioning values will influence both absolute and relative abundances (REE profile slopes), and therefore have a profound effect on the proportions of crystal-liquid mixture, rendering them largely arbitrary, particularly without a geologically constrained parent magma composition to being with. A plot of P against Ce (Fig. 9) shows a general alignment through the origin towards liquid-like values, as represented by olivine diabase of the Sudbury Dykes, suggesting that the REE variation could be consistent with variability in trapped liquid contents. Given the lack of constraint, no further quantification of these mixtures will be attempted here. The significant scatter also suggests that other factors, such as contamination and/or metamorphic redistribution may also have affected the geochemical distributions.

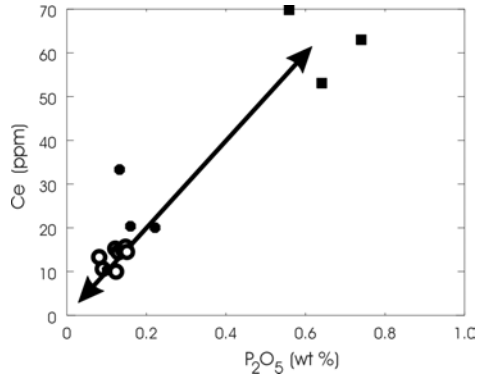

Figure 9: P_2O_5 - *Ce plot.*

The consistency of the normalised trace element distributions (Fig. 5) suggests that there has not been significant compositional redistribution by metamorphism on the whole-rock scale, and the relative abundance patterns can be readily attributed to plagioclase accumulation. While no independently constrained parent liquid compositions exist for the anorthosites, the Sudbury Dykes represent approximately contemporaneous, geographically proximal mantle-derived materials. REE and spidergram plots (Fig. 5) indicate that the Sudbury Dykes are, unsurprisingly, incompatible-element enriched and less fractionated than the anorthosites. While there is no direct relationship between these dykes and the anorthosites, and the dykes are unlikely to represent unfractionated liquids, they do appear to provide a useful reference composition against which the compositional effects of plagioclase accumulation can be qualitatively estimated.

For example, plots of CaO against Y have been devised to discriminate fractionation trends in mafic volcanic liquids (Lambert and Holland, 1974), and can be used to distinguish the effects of fractionation of plagioclase, pyroxene and amphibole. Figure 10A shows the St Charles and Mercer samples on this plot. Vectors can be calculated for plagioclase fractionation and accumulation, using partition coefficients for Y in plagioclase, Ca-content appropriate to the plagioclase of choice (An_{55} used, consistent with the normative compositions), and finally, a starting composition. In Figure 10A, a starting composition has been approximated using the general basaltic parent liquid composition provided by Lambert and Holland (1976), as well as Sudbury Dyke olivine diabase values (Condie et al., 1987). The anorthosite whole-rock

compositions plot very conveniently as products of accumulation of andesine plagioclase from starting compositions comparable to those plotted. Similarly (or conversely), the Sudbury Dyke samples appear to demonstrate the effects of a liquid which has lost variable amounts of plagioclase, suggesting that they do, in fact, represent fractionated liquids rather than primitive parents. Scatter amongst the anorthosite samples may represent the effects of clinopyroxene addition, or of a separate process such as contamination.

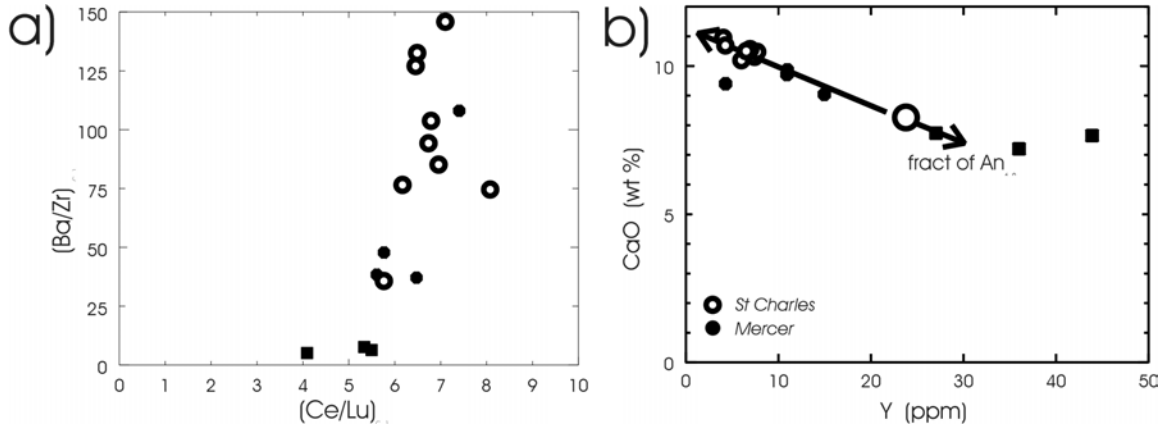

Figure 10: *CaO-Y and Ba/Zr-Ce/Lu plots.*

Plots involving major elements, compatible trace elements, incompatible trace elements, and isotopic variations therein are progressively more sensitive (in that sequence) to the effects of contamination. A plot of Ba/Zr ratio against Ce/Lu can be used to monitor the effects of plagioclase abundance variation, as shown in Figure 10B. Ba and the LREE are more compatible in calcic plagioclase than are Zr and the HREE, as is apparent from the spidergram shown previously (Fig. 5B). A calculated plagioclase composition from an average Sudbury Dyke would have a $(Ba/Zr)_{PM}$ ratio around 250, and a $(Ce/Lu)_{CH}$ ratio around 7.7. The anorthosite samples plot on, or to the right of, a line which would reflect variable mixtures of feldspar and liquid. Pyroxenes would plot with lower values of both indices, to the lower left. As suggested on the basis of REE abundances and Eu anomalies, the Mercer samples appear to show larger liquid contributions, on average, than do the St Charles samples. Contamination by LREE-enriched continental crust would push the samples to the lower right, consistent with the distribution pattern observed. The heterogeneity of local supracrustal rock compositions preclude meaningful quantitative constraints of the contamination based on these data.

By combining REE abundances with radiogenic isotopic compositions, a more sensitive indicator of contamination can be derived. There are no systematic compositional differences between the *c.* 1900 Ma and the *c.* 2700 Ma gneisses (based on Nd model age) in terms of elemental abundances (Dickin and McNutt, 1990), but their isotopic compositions are distinct (by definition). Figure 11 shows Nd abundance plotted against ε_{Nd}^{1240} for the anorthosite samples, with fields for the two local crustal reservoirs also shown. Using a starting composition with 5 ppm Nd and $\varepsilon_{Nd}^{1240} = 0$, the two anorthosites fall onto two very distinct trends, whereby the St Charles samples lie along a trend defined by contamination with Archaean crust, while the Mercer samples lie on the trend for contamination by the Proterozoic crust. If a depleted mantle starting composition is used (e.g., with ε_{Nd}^{1240} of around +5 and very low Nd abundance), the amount of contamination required is quite a bit higher, and the anorthosite samples do not fit the mixing curves. However, there seems to be no direct evidence of the existence of isotopically depleted mantle magmas found in Proterozoic mafic rocks from Ontario to Labrador, such that

the most depleted samples measured are isotopically chondritic (i.e., $\varepsilon_{Nd}^{i} = 0$). This being the case, there is no basis for a depleted mantle starting composition, and the one chosen is consistent with available data.

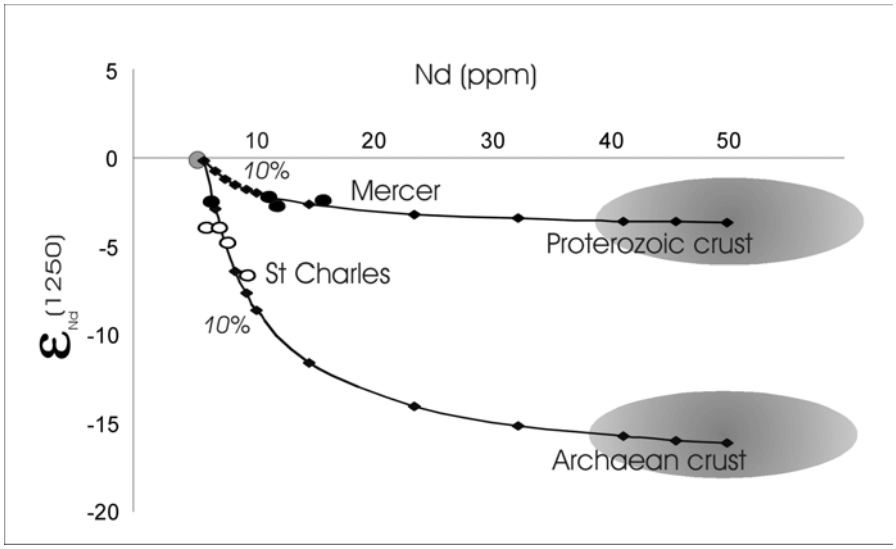

Figure 11: *Nd abundance vs. isotopic composition, demonstrating mixing with compositionally similar, but different-aged reservoirs, corresponding to the expected basement compositions (from Dickin and McNutt, 1990)*

While the isotopic composition of the anorthosites would be unaffected by variations in crystal/liquid proportions, the Nd abundance would be. Given the relatively limited extent of mineralogical variation in the anorthosites (from 79 to 90 normative percentage feldspar), this suggests limited variation in crystal-liquid proportions. Without real constraints on liquid compositions, this cannot be well constrained, but 10% addition of a basaltic liquid with 40 ppm Nd (Sudbury Dykes have average Nd around 40 ppm, estimated from Condie et al. [1987] assuming a basaltic-type Nd/Sm ratio around 5.5) would change Nd abundances from 15 ppm in a plagioclase cumulate to about 18 ppm in a cumulate-liquid mixture. Therefore, the quantities of crustal contamination modelled on this diagram must be viewed as somewhat qualitative, particularly in the case of the Mercer samples, where isotopic compositions are relatively constant, and the apparent mixing is constrained exclusively by the Nd abundance variation. This is less the case for the St Charles suite. This clear distinction and the lack of significant isotopic overlap also supports a model of contamination by isotopically distinct crustal reservoirs, even with such a small database. The geochemical variation diagrams do not suggest that the Mercer samples were either significantly less contaminated (i.e., significantly more rigorously compositionally controlled by fractional crystallisation) nor significantly less prone to reflecting this contamination (e.g., such as by virtue of having dramatically elevated REE abundances, which could have buffered the effects of contamination, effectively).

Therefore, while the major and compatible trace element variation in the anorthosites is consistent with control by relatively small differences in the proportions of plagioclase and associated liquid, the Sm-Nd isotopic evidence indicates not only small and variable amounts of crustal contamination, but that the two intrusions sampled isotopically distinct contaminants. Since the intrusions are both hosted by the West Bay Pluton, it is very unlikely (although perhaps not impossible) that the contamination occurred during final emplacement in the upper crustal granitoid, and must have occurred previously at depth. The isotopic modelling is consistent with the model-age terrane boundary indicated by Dickin (2000), such that the St Charles Anorthosite shows Archaean contamination north of the boundary, and the Mercer Anorthosite shows

Proterozoic contamination on the south side. This indicates that the contamination occurred at a crustal level below the granitoid. The isotopic heterogeneity of the contaminated rocks, specifically the St Charles samples, is not particularly consistent with contamination in a lower crustal subchamber, such as where an olivine basaltic primary liquid might have crystallised plagioclase to form a floating anorthositic mush, subsequently emplaced upwards (re. Ashwal, 1993), and where distinct but homogeneous isotopic signatures might be expected. These, albeit limited, data, rather favour a more progressive differentiation and fractionation process whereby early contaminated batches of partially crystallised magma (mushes) could be emplaced and cooled, in part, prior to isotopic equilibration or homogenisation with earlier or later batches.

TECTONIC IMPLICATIONS

While the scope and scale of this study are far too small to shed much light on the nature of the relationship between the West Bay Batholith and the St Charles and Mercer anorthosites, the association of the granites and anorthosites, their apparent similar deformational history, and the age data (unpublished for the former intrusion and poorly constrained for the latter two) are all consistent with a possible anorthosite-mangerite-charnockite-granite (AMCG) suite (e.g., Emslie and Hegner, 1993). A *c*. 1240 Ma AMCG suite in the Grenville of western Ontario is consistent with the age and geographic distribution of Proterozoic massif-type anorthosites (e.g., Wiebe, 1992), but is of no special significance in this regard. In general, the emplacement of anorthosite massifs has been associated with stable, cratonic terranes (e.g., Wiebe, 1992; Ashwal, 1993), which has led to their classification as so-called anorogenic magmatism. However, detailed mapping, and geochronological and isotopic studies over the past twenty years or so (such as those presented in the introduction) have revealed that many anorthositic magmatic suites are closely associated with previously unrecognised crustal sutures and terrane boundaries. Gower and Krogh (2002) have suggested a relationship between anorthosite massifs in Labrador and the activity of flat subduction, produced by subduction of a thickened oceanic crust, perhaps by the occurrence of oceanic plateaus, to produce orogenic magmatic activity well inboard (up to several hundred kilometres, according to Gutscher et al. [2000]) of the actual subduction front. This would account for linear magmatic belts, which are not obviously related to proximal subduction tectonics.

A *c.* 1240 Ma age for the Burwash anorthosites is contemporaneous with the closure of the Bancroft, Elsevier, and Sharbot Lake Terranes of the Central Metasedimentary Gneiss Belt (CMGB), 300 km or so to the southeast. A variety of tectonic models have been expounded for the formation of the CMGB (in contrast to the relatively limited selection for the Central Gneiss Belt, which are dominated by continental collision and thrusting), effectively summarized by Easton (1992). These include both rift-based and island arc-based models. It is perhaps worth noting that Dickin and McNutt (1989) also favoured an island-arc accretion model for the Central Gneiss Belt. The apparent absence of post-1240 Ma magmatism in the CMGB terranes suggests that, whatever their tectonic environments of formation, they were behaving as a coherent cratonic entity by 1240 Ma, subsequently to be affected by Grenvillian metamorphic overprinting. The closure of the Bancroft, Elsevier, and Sharbot Lake Terranes is marked by primarily felsic (granitic) plutonism, in contrast to the mafic plus felsic AMGC plutonism and the mafic dykes, progressively further north. This temporal association of distal mafic rocks with a geographically distinct, otherwise granitic orogenic event has also been observed in the *c*. 1750 Ma Killarnean Orogeny (Prevec, 1995), and may reflect the existence of a more distal extensional regime, which is induced or complemented by compressional tectonics and crustal melting at the orogenic locus.

ECONOMIC IMPLICATIONS

Although anorthositic rocks, in particular, and AMCG suites in general, have not been traditionally associated with economically viable ore deposits (apart from quarry stone), the relatively recent advent of the massive Voisey's Bay Cu-Ni sulphide deposit in eastern Labrador, Canada, inspired world-wide economic exploration interest in these rocks, yet to be justified by subsequent exploration. The Voisey's Bay deposit lies near the southern end of the Nain Anorthosite Suite, approximately overlying the Palaeoproterozoic boundary between the Archaean Nain and Neoarchaean-Palaeoproterozoic Churchill (Rae) Provinces, about 300 km north of the *c.* 1000 Ma Grenville Front (Ryan et al., 1995). Whether this has any direct relevance to the occurrence or the preservation of the Voisey's Bay deposit is purely speculative, but the role of upper and lower crust, and the nature of the upwelling mantle proximal to crustal terrane boundaries may well be significant, particularly in light of the apparent uniqueness of this deposit. Significant Cu-Ni-PGE sulphide-bearing leucogabbroic rocks occur along rift zones in the Palaeoproterozoic in Canada, Finland and Russia. Identification of deformed equivalents of these rifted terrane boundaries hosting similar mineralisation could be conducted using isotopic systematics in their anorthositic components, potentially leading to new ore discoveries.

SUMMARY AND CONCLUSIONS

The occurrence of AMGC suites across terrane boundaries in Labrador and Ontario has provided a potential upper-crustal discriminant for lower crustal structures. The dominantly monomineralic massif-type anorthosites in the Burwash area (Lumbers, 1975) are characterised by similarities in:

(1) field relationships, where both are hosted by the West Bay Batholith, and have been affected by the same large scale deformations as their host rock;

(2) age, at *c.* 1240 Ma;

(3) petrology, comprising 85-92 normative % sodic labradorite (An_{5x}), with metamorphic grade reflecting prograde amphibolite facies; and

(4) geochemistry, showing control of the major and trace elements by differing proportions of plagioclase feldspar and liquid, with minor scatter attributable to other factors, such as contamination or pyroxene fractionation.

The two anorthosites are notably different only in terms of:

(1) their position within the granite relative to the location of the northern margin of Barilia, as mapped on the basis on Nd model ages (Dickin, 2000), whereby the St Charles Anorthosite lies to the north of the revised boundary and the Mercer Anorthosite to the south; and

(2) Sm-Nd isotopic composition, where the St Charles and Mercer anorthosites reflect small amounts (<10%) of contamination by Archaean and Proterozoic basement, respectively.

From this, it may be concluded that the apparent terrane boundary reflected by the Nd model age break in the supracrustal gneisses is also represented in the anorthosites, in particular, and in the AMCG complex, in general, which have intruded the gneisses. This indicates that the isotopic

break exists at depth, as well as in the upper crust, and does, in fact, represent a probable terrane boundary, as opposed, for example, to supracrustal mixing of isotopically distinct reservoirs. This further indicates an association between the AMCG suite and a terrane boundary, as distinct from an intracratonic (intraterrane) "anorogenic" environment. Finally, this appears to represent part of the process of terrane assembly in the Central Gneiss and Central Metasedimentary Belts of the Ontario Grenville Province, which concluded at *c.* 1240 Ma, prior to subsequent thrusting as a coherent entity at *c.* 1000 Ma and with which the Grenville Province as a whole is associated.

ACKNOWLEDGEMENTS

Bud Baadsgaard is acknowledged for his involvement in the very earliest stages of this research, as well as for conducting the SHRIMP analyses at Canberra during his sabbatical there in 1990. Ian Williams is acknowledged for humouring Bud and accommodating said analyses. The farmer who rescued us from the mud with his tractor in Mercer Township, and then provided us with about two pounds of bacon as change for a $20 bill, is very gratefully acknowledged. Financial support for trace element geochemical analyses from the University of the Witwatersrand through a University Research Council grant is acknowledged.

REFERENCES

Ashwal, L.D. (1993). *Anorthosites.* Springer-Verlag Berlin ,422 pp.

Ashwal, L.D. and Wooden, J.L. (1983). Isotopic evidence from the eastern Canadian Shield for geochemical discontinuity in the Proterozoic mantle. Nature, 306, 679-680.

Ashwal, L.D., Wooden, J.L. and Emslie, R.F. (1986). Sr, Nd, and Pb isotopes in Proterozoic intrusives astride the Grenville Front in Labrador: implications for crustal contamination and basement mapping. Geochimica et Cosmochimica Acta, 50, 2571-2585.

Chen, Y.D., Krogh, T.E. and Lumbers, S.B. (1995). Neoarchean trondhjemitic and tonalitic orthogneisses identified within the northern Grenville Province in Ontario by precise U-Pb dating and petrologic studies. Precambrian Research, 72, 263-281.

Condie, K.C., Bobrow, D.J. and Card, K.D. (1987). Geochemistry of Precambrian mafic dykes from the southern Superior Province of the Canadian Shield *In: Mafic Dyke Swarms* (edited by H.C. Halls and W.F. Fahrig), Geological Association of Canada Special Paper 34, 95-108.

Davidson, A. (1986). New interpretations in the southwestern Grenville Province *In*: The Grenville Province, edited by J.M. Moore, A. Davidson and A.J. Baer, Geological Association of Canada Special Paper 31, 61-74.

Dickin, A.P. (1998a). Nd isotope mapping of a cryptic continental suture, Grenville Province of Ontario. Precambrian Research, 91, 433-444.

Dickin, A.P. (1998b). Pb isotope mapping of differentially uplifted Archean basement: a case study from the Grenville Province, Ontario. Precambrian Research, 91, 445-454.

Dickin, A.P. (2000) Crustal formation in the Grenville Province: Nd-isotope evidence. Canadian Journal of Earth Sciences, 37, 165-181.

Dickin, A.P. and McNutt, R.H. (1989). Nd model age mapping of the southeast margin of the Archean Foreland in the Grenville Province of Ontario. Geology, 17, 299-301.

Dickin, A.P. and McNutt, R.H. (1990). Nd model-age mapping of Grenville lithotectonic domains: mid-Proterozoic crustal evolution in Ontario *In: Mid-Proterozoic Laurentia Baltica*, edited by C.F. Gower, T. Rivers and A.B. Ryan, Geological Association of Canada Special Paper 38, 79-94.

Dickin, A.P., McNutt, R.H. and Clifford, P.M. (1990). A neodymium isotope study of plutons near the Grenville Front in Ontario, Canada. Chemical Geology, 83, 315-324.

Easton, R.M. (1986). Geochronology of the Grenville Province *In* : *The Grenville Province,* edited by J.M. Moore, A. Davidson and A.J. Baer, Geological Association of Canada Special Paper 31, 127-174.

Easton, R.M. (1992). The Grenville Province and the Proterozoic history of central and southern Ontario *In*: *Geology of Ontario*, Ontario Geological Survey Special Volume 4, Part 2, p. 715-904.

Emslie, R.F. and Hegner, E. (1993). Reconnaisance isotopic geochemistry of anorthosite-mangerite-charnockite-granite (AMCG) complexes, Grenville Province, Canada. Chemical Geology, 106, 279-298.

Emslie, R.F. and Hunt, P.A. (1989). Ages and petrogenetic significance of igneous mangerite-charnockite suites associated with massif anorthosites, Grenville Province. Journal of Geology, 98, 213-231.

Emslie, R.F., Hamilton, M.A. and Therriault, R.J. (1994). Petrogenesis of a mid-Proterozoic Anorthosite-Mangerite-Charnockite-Granite (AMCG) Complex: isotopic and chemical evidence from the Nain Plutonic Suite. Journal of Geology, 102, 539-558.

Fahrig, W.F. (1987). The tectonic settings of continental mafic dyke swarms: failed arm and early passive margin *In:* *Mafic Dyke Swarms* (edited by H.C. Halls and W.F. Fahrig), Geological Association of Canada Special Paper 34, 331-348.

Gower, C.F. and Krogh, T.E. (2002). A U-Pb geochronological review of the Proterozoic history of the eastern Grenville Province. Canadian Journal of Earth Sciences, 39, 795-829.

Guo, A. and Dickin, A.P. (1996). The southern limit and Archean crust and significance of rocks with Paleoproterozoic model ages: Md model age mapping in the Grenville Province of western Quebec. Precambrian Research, 77, 231-241.

Gutscher, M.-A., Spakman, W., Bijwaard, H. and Engdahl, E.R. (2000). Geodynamics of flat subduction: seismicity and tomographic constraints from the Andean margin. Tectonics, 19, 814-833.

Holmden, C. and Dickin A.P. (1995). Paleoproterozoic crustal history of the southwestern Grenville Province: evidence from Nd isotopic mapping. Canadian Journal of Earth Sciences, 32, 472-485.

Krogh, T.E., Corfu, F., Davis, D.W., Dunning, G.R., Heaman, L.M., Kamo, S.L., Machado, N., Greenough, J.D. and Nakamura, E. (1987). Precise U-Pb isotopic ages of diabase dykes and mafic to ultramafic rocks using trace amounts of baddeleyite and zircon *In* : *Mafic Dyke Swarms* (edited by H.C. Halls and W.F. Fahrig), Geological Association of Canada Special Paper 34: 147-152.

Lambert, R.St.J. and Holland, J.G. (1974). Yttrium geochemistry applied to petrogenesis utilizing calcium-yttrium relationships in minerals and rocks. Geochimica et Cosmochimica Acta, 38, 1393-1414.

Lumbers, S.B. (1975). Geology of the Burwash Area, Districts of Nipissing, Parry Sound, and Sudbury. Ontario Division of Mines Geological Report 116, 158 pp. + map 2271.

Lumbers, S.B., Wu, T.-W., Heaman, L.M., Vertolli, V.M. and MacRae, N.D. (1991). Petrology and age of the A-type Mulock granite batholith, northern Grenville Province, Ontario. Precambrian Research, 199-231.

Osmani, A. (1991). Proterozoic mafic dyke swarms in the Superior Province of Ontario *In:* *Geology of Ontario,* Ontario Geological Survey Special Volume 4, Part 1, 661-681.

Phinney, W.C. and Morrison, D.A. (1990). Partition coefficients for calcic plagioclase: implications for Archean anorthosites. Geochimica et Cosmochimica Acta, 54, p. 1639-1654.

Prevec, S.A. (1993). *An isotopic, geochemical and petrographic investigation of the genesis of Early Proterozoic mafic intrusions and associated volcanism near Sudbury, Ontario*, Ph.D. thesis (unpubl.), University of Alberta, Edmonton, Alberta, 165 p. plus appendices.

Prevec, S.A. (1995). Sm-Nd isotopic evidence for crustal contamination in the ca. 1750 Ma

Wanapitei Complex, western Grenville Province, Ontario. Canadian Journal of Earth Science, 32, p. 486-495.
Prevec, S.A. (2000). An examination of modal variation mechanisms in the contact sublayer of the Sudbury Igneous Complex, Canada. Mineralogy and Petrology, 68, p. 141-157.
Rivers, T. (1997). Lithotectonic elements of the Grenville Province: review and tectonic implications. Precambrian Research, 86, 117-154.
River, T. and Corrigan, D. (2000). Convergent margin on southeastern Laurentia during the Mesoproterozoic: tectonic implications. Canadian Journal of Earth Sciences, 37, 359-383.
Rivers, T., Martignole, J., Gower, C.F. and Davidson, A. (1989). New tectonic divisions of the Grenville Province, southeast Canadian Shield. Tectonics, 8, 63-84.
Rousell, D.H. (1978). Geology of the anorthositic sill at St. Charles, Ontario *In* : Current Research, Part A, Geological Survey of Canada, Paper 78-1A, 163-168.
Rousell, D.H. (1981). Fabric and origin of gneissic layers in anorthositic rocks of the St. Charles sill, Ontario. Canadian Journal of Earth Sciences, 18, 1681-1693.
Ryan, B., Wardle, R., Gower, C. and Nunn, G. (1995). Nickel-copper-sulphide mineralization in Labrador: the Voisey Bay discovery and its exploration implications. Current Research, Newfoundland Department of Natural Resources, Report 95-1, 177-204.
Simmons, E.C. and Hanson, G.N. (1978). Geochemistry and origin of massif-type anorthosites. Contributions to Mineralogy and Petrology, 66, 119-135.
Simmons, E.C., Hanson, G.N. and Lumbers, S.B. (1980). Geochemistry of the Shawmere Anorthosite Complex, Kapuskasing Structural Zone, Ontario. Precambrian Research, 11, 43-71.
Stockwell, C.H. (1969). Structural provinces, orogenies, and time-classifications of rocks of the Canadian Shield; Age determinations by the Geological Survey of Canada. Report 2, Isotopic Ages: Geological Survey of Canada Paper 61-17, 108-118.
van Breemen, O., Davidson, A., Loveridge, W.D. and Sullivan, R.W. (1986). U-Pb zircon geochronology of Grenville tectonites, granulites and igneous precursors, Parry Sound, Ontario *In: The Grenville Province*, edited by J.M. Moore, A. Davidson and A.J. Baer, Geological Association of Canada Special Paper 31, 191-207.
Wiebe, R.A. (1992). Proterozoic anorthosite complexes *In: Proterozoic Crustal Evolution, Developments in Precambrian Geology 10*, edited by K.C. Condie, Elsevier, 215-261.
Wynne-Edwards, H.R. (1972). The Grenville Province *In: Variations in Tectonic Styles in Canada*, edited by R.A. Price and R.J.W. Douglas, Geological Association of Canada Special Paper 11, 263-334.

_____oOo_____